A New Neutron Time-of-Flight Detector for Fuel-Areal-Density Measurements on OMEGA

The areal density of the compressed core is an important observable in inertial confinement fusion[1] (ICF) experiments. The most-common method to infer the fuel areal density in cryogenic deuterium–tritium (DT) implosions uses the primary 14.1-MeV neutrons that elastically scatter off the deuterons and tritons in the dense shell surrounding the hot spot.[2] There are two independent diagnostics on OMEGA[3] to measure the fuel areal density. The first one is the magnetic recoil spectrometer (MRS),[4] which measures the forward-scattered neutron spectrum between 10 and 12 MeV. The second is a neutron time-of-flight (nTOF) detector in a well-collimated line of sight (LOS), which measures backscattered neutrons[5] between 1 and 6 MeV. Simultaneous fuel-areal-density measurements by the MRS and nTOF, which view the target from different directions, make it possible to study implosion asymmetries on OMEGA. This article describes recent improvements and modifications to the nTOF system for the fuel areal density on OMEGA.

A neutron time-of-flight spectrum for a cryogenic DT implosion with an areal density of 220 mg/cm^2 and a T_i of 2.4 keV for a detector at 13.4 m from the target is shown in Fig. 139.49. This spectrum was generated using one-dimensional (1-D) *LILAC*[6] simulations and post-processed in *IRIS*.[7] The spectrum consists of at least six separate neutron contributions and has a dynamic range of 10^6. The dominant DT peak is estimated to deposit more than 90% of the neutron energy into a scintillator-based nTOF detector. Such a large signal may saturate the photomultiplier tube (PMT) and produce a long light-afterglow component in the scintillator.[8] At least four gated PMT's with different sensitivities are required to cover the full dynamic range of the entire neutron spectrum.

To mitigate the long light-afterglow component, advanced scintillating compounds were developed including a liquid scintillator based on oxygenated xylene[9] and a solid bibenzyl crystal.[10] The maximum diameter of the scintillator cavity (8 in.) is determined by the maximum available distance from the target on OMEGA (13.4 m) and the diameter of the hole in the concrete floor of the Target Bay that is used as a second collimator.[5] The thickness of the scintillator cavity was chosen

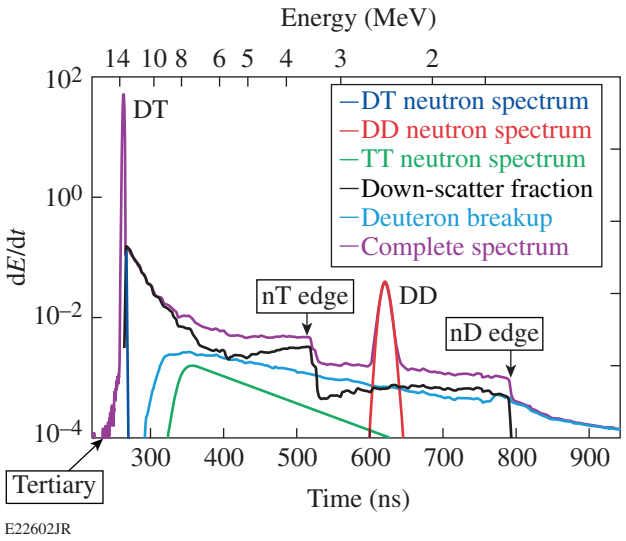

Figure 139.49
A neutron time-of-flight spectrum is generated for a cryogenic DT implosions on OMEGA.

to be 4 in. to ensure adequate neutron statistics for the yields available with cryogenic DT shots on OMEGA.

The new 8 × 4 nTOF detector is a modification and improvement of the nTOF20-Spec detectors[11] for the National Ignition Facility (NIF) and 6 × 2 nTOF detector[5] on OMEGA. The number of PMT's was increased from two to four; the scintillator volume was increased by a factor of 2.7; the mass of material in the detector body was decreased as much as possible; and compartments for neutral-density filters between windows and PMT's were eliminated. A computer-aided design (CAD) model of the new 8 × 4 nTOF detector is shown in Fig. 139.50. The main part of the detector is a thin-wall, stainless-steel scintillator cavity with five holes machined from a single piece of metal. The inside cavity dimensions are 8 in. diameter by 4 in. thick. To decrease the chemical-reaction surface area, the cavity and thin stainless-steel covers were electropolished after manufacturing. The four larger holes have 50-mm fused-silica windows. Four PMT housings were designed to accommodate Photek[12] PMT240 or PMT140 gated microchannel plate (MCP)

photomultipliers with a 40-mm photocathode. The 3-cm hole on the top is used to fill the cavity with a scintillator and is covered with an expansion bellows after filling. Two flat stainless-steel covers seal the scintillator cavity on the front and back of the detector. For ion-temperature measurements, optional indented covers can be used instead, thereby reducing the scintillator thickness from 10 to 5 cm.

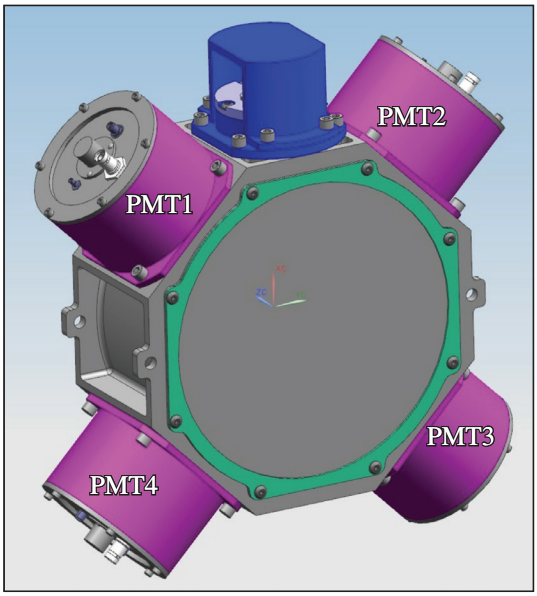

Figure 139.50
A computer model of the 8 × 4 nTOF detector.

The 8 × 4 nTOF is mounted to the ceiling beneath the Target Bay at 13.4 m from the target. The mid-beam collimator[5] was modified to project a 19-cm-diam neutron beam to the face of the 8 × 4 nTOF detector. To decrease neutron scattering, the 20-mm-thick quartz vacuum window to the target chamber was replaced by a 1.9-mm stainless-steel window.

One PMT140 and three PMT240's were installed on the 8 × 4 nTOF. The low-gain PMT140 measures the primary DT neutron signal; the first PMT240 measures DT areal density in the nT-edge region from 1.5 to 6 MeV, the second PMT240 measures DT areal density in the nD-edge region below 2-MeV, and the third PMT240 is used for testing. We use the most-recent fast-gated Photek PMT240's with a meshed photocathode and fast GM300-8U gate units that together provide a gate recovery time of about 15 ns. The signals from each of the four PMT's are transmitted by 6-m-long LMR-600 cables to four 1-GHz, 10-GS/s Tektronix DPO7104 oscilloscopes. A resistive splitter divides the PMT signal into four oscilloscope channels with different sensitivity settings to increase the dynamic range of the recording system.

The primary DT neutrons are measured by the ungated PMT140 with a gain of 50. Figure 139.51 shows the typical scope trace of the neutron signal from the PMT140 taken for a cryogenic shot with a DT yield of 2.3×10^{13}. The signal in Fig. 139.51 was fitted by a convolution[13] of a Gaussian and exponential scintillator decay to calculate the total charge. Such a fit approximates the measured signal very well without any rescattering tails. This 8 × 4 nTOF detector channel was calibrated for a primary DT yield against the 12-m nTOF-H detector[14] with a statistical precision of 3.5% rms (root mean square).

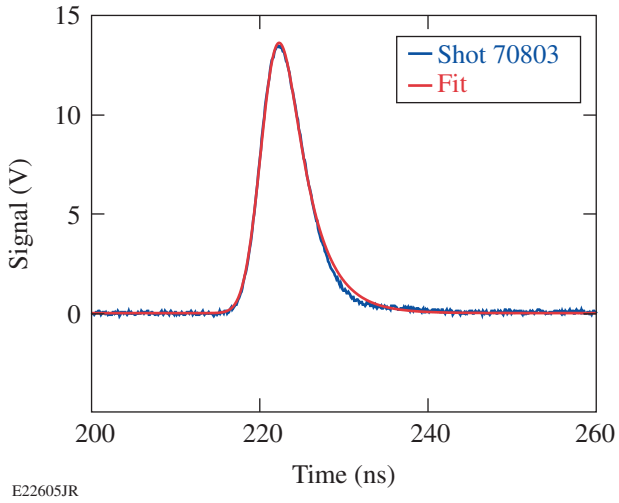

Figure 139.51
Neutron signal recorded for the PMT140 on a DT shot with a yield of 2.3×10^{13}.

Figure 139.52 shows the scope traces from the PMT240 with a gain of 400 for three cryogenic shots in the nT-edge region, normalized to the primary DT yield. The DT neutron peak was gated out; the small peak at 215 ns is a result of direct interactions of rescattered neutrons with the MCP's in the PMT. The gate was turned off at 300 ns for two of the shots and at 320 ns for the third shot. The nT edge at ~470 ns is clearly visible, as is the difference in areal density between shots. An analysis of these shots, as described in Ref. 5, produced areal densities of 165 mg/cm^2, 124 mg/cm^2, and 174 mg/cm^2. The nD edge at 730 ns is barely visible in Fig. 139.52.

A scope trace from a different PMT240 with a gain 1×10^4 for an nD-edge region measurement is shown in Fig. 139.53. The gate-out region for this PMT was extended to the end of the DD neutron peak at 600 ns (see Fig. 139.52). The PMT can

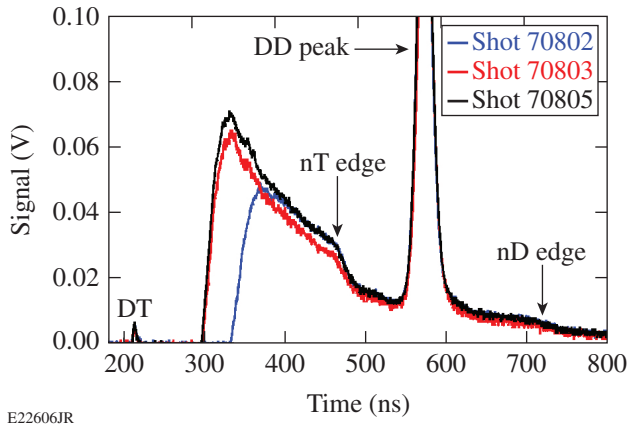

Figure 139.52
Neutron signal recorded for the gated PMT240 on DT cryogenic shots 70802, 70803, and 70805.

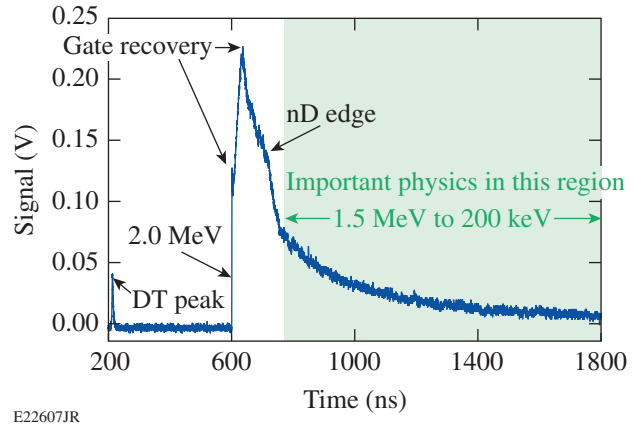

Figure 139.53
Neutron signal recorded for the gated PMT240 on DT cryogenic shot 69239 with a yield of 1.8×10^{13}.

be operated at a much higher gain if the primary DD peak is eliminated with the gate. As in Fig. 139.52, the direct interaction of DT neutrons with the MCP can be seen at 215 ns; gate recovery can be seen from 600 ns to 615 ns, and the nD edge is now clearly visible at 730 ns. The areal density from the nD edge is inferred based on an analysis similar to that used for the nT edge. Recent areal-density measurements from the nT- and nD-edge regions are compared in Table 139.IV. There is good agreement between areal densities measured in nT- and nD-edge regions. The signal below the nD edge (1.56 MeV) consists of the residual neutron-scattering background, T–T reactions, and a deuteron breakup reaction. All these contributions are currently under study.

Table 139.IV: Comparison of areal densities measured in nT- and nD-edge regions.

Shot number	nT areal density (mg/cm^2)	nD areal density (mg/cm^2)
71527	158	166
71528	180	177
71529	166	175
71530	187	179

The fourth PMT was used to investigate the possibility of measuring tertiary[15] neutrons with energies larger than the primary 14.06-MeV neutrons. The yield of the tertiary neutrons is about 10^{-6} from the primary D–T yield and they appear just before the rising edge of the DT peak. To record tertiary neutrons, a high-gain PMT is needed that is sensitive only during the short arrival time window before the DT peak. The most-recent Photek PMT's have a normally off-gating option that is ideal for tertiary neutron measurements. Figure 139.54 shows raw scope traces from the PMT240 with a gain of 10^6 that were recorded on three different shots using the same PMT, scope, and different gate timing. Shot 69233 (blue trace) was recorded in the normally on-gating option in an x-ray–producing shot and shows the position of the x-ray peak in time. Shot 69236 (red trace) was recorded in the normally off-gating mode without any gate pulse and showed the position of the DT peak from direct interaction of neutrons with the MCP at 220 ns. Shot 69242, with a primary yield of 1.8×10^{13}, was recorded with the normally off-gating mode and a 160-ns-wide gate-opening pulse. Figure 139.54 shows that the gate eliminates the hard x rays and most of the DT pulse. The rising edge of the DT pulse saturates the scope after 215 ns, causing oscillation in the signal. However, the scope survives and is fully operational after several similar tests. The data at

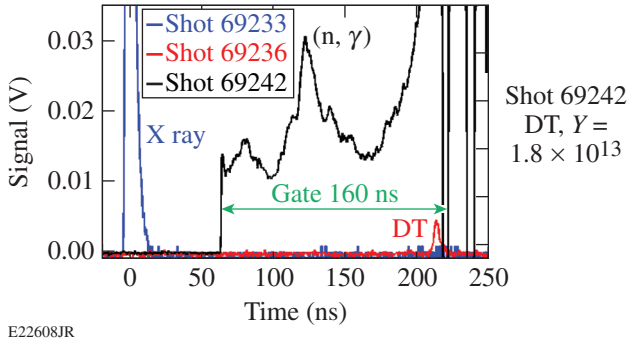

Figure 139.54
X-ray and neutron signals recorded for the normally off-gated PMT240 with a gain of 10^6 on shots 69233, 69236, and 69242.

~180 ns (shown in Fig. 139.54) are most probably from neutron interactions with structures in the target area. The technical ability to measure neutrons with an energy of more than 14 MeV was demonstrated using the nTOF technique. Tertiary measurements on OMEGA are extremely difficult because the areal density is relatively low and the 8 × 4 nTOF detector is not sufficiently shielded from gammas. On the NIF, where yields and areal densities are higher and the nTOF detectors in the "neutron alcove" are well-shielded, the situation is much more favorable.

The new 8 × 4 nTOF detector with four gated PMT's each with different gains makes it possible for the primary DT and D_2 neutrons to be measured on the same shot on the same LOS. Fuel areal densities can be inferred from down-scattered neutrons in the nT- and nD-edge regions, and tertiary neutrons can be studied using the same detector. The 8 × 4 nTOF is now the main detector for areal-density measurements on OMEGA.

ACKNOWLEDGMENT

This work was partially supported by the Department of Energy National Nuclear Security Administration under Award No. DE-NA0001944, the University of Rochester, and the New York State Energy Research and Development Authority. The support of DOE does not constitute an endorsement by DOE of the views expressed in this article.

REFERENCES

1. J. D. Lindl, *Inertial Confinement Fusion: The Quest for Ignition and Energy Gain Using Indirect Drive* (Springer-Verlag, New York, 1998).
2. C. D. Zhou and R. Betti, Phys. Plasmas **15**, 102707 (2008).
3. T. R. Boehly, D. L. Brown, R. S. Craxton, R. L. Keck, J. P. Knauer, J. H. Kelly, T. J. Kessler, S. A. Kumpan, S. J. Loucks, S. A. Letzring, F. J. Marshall, R. L. McCrory, S. F. B. Morse, W. Seka, J. M. Soures, and C. P. Verdon, Opt. Commun. **133**, 495 (1997).
4. J. A. Frenje, D. T. Casey, C. K. Li, J. R. Rygg, F. H. Séguin, R. D. Petrasso, V. Yu. Glebov, D. D. Meyerhofer, T. C. Sangster, S. Hatchett, S. Haan, C. Cerjan, O. Landen, M. Moran, P. Song, D. C. Wilson, and R. J. Leeper, Rev. Sci. Instrum. **79**, 10E502 (2008).
5. C. J. Forrest, P. B. Radha, V. Yu. Glebov, V. N. Goncharov, J. P. Knauer, A. Pruyne, M. Romanofsky, T. C. Sangster, M. J. Shoup III, C. Stoeckl, D. T. Casey, M. Gatu-Johnson, and S. Gardner, Rev. Sci. Instrum. **83**, 10D919 (2012).
6. J. Delettrez, R. Epstein, M. C. Richardson, P. A. Jaanimagi, and B. L. Henke, Phys. Rev. A **36**, 3926 (1987).
7. P. B. Radha, J. A. Delettrez, R. Epstein, S. Skupsky, J. M. Soures, S. Cremer, and R. D. Petrasso, Bull. Am. Phys. Soc. **44**, 194 (1999).
8. C. Stoeckl, M. Cruz, V. Yu. Glebov, J. P. Knauer, R. Lauck, K. Marshall, C. Mileham, T. C. Sangster, and W. Theobald, Rev. Sci. Instrum. **81**, 10D302 (2010).
9. R. Lauck *et al*., IEEE Trans. Nucl. Sci. **56**, 989 (2009).
10. V. Yu. Glebov, C. Forrest, J. P. Knauer, A. Pruyne, M. Romanofsky, T. C. Sangster, M. J. Shoup III, C. Stoeckl, J. A. Caggiano, M. L. Carman, T. J. Clancy, R. Hatarik, J. McNaney, and N. P. Zaitseva, Rev. Sci. Instrum. **83**, 10D309 (2012).
11. V. Yu. Glebov, T. C. Sangster, C. Stoeckl, J. P. Knauer, W. Theobald, K. L. Marshall, M. J. Shoup III, T. Buczek, M. Cruz, T. Duffy, M. Romanofsky, M. Fox, A. Pruyne, M. J. Moran, R. A. Lerche, J. McNaney, J. D. Kilkenny, M. J. Eckart, D. Schneider, D. Munro, W. Stoeffl, R. Zacharias, J. J. Haslam, T. Clancy, M. Yeoman, D. Warwas, C. J. Horsfield, J.-L. Bourgade, O. Landoas, L. Disdier, G. A. Chandler, and R. J. Leeper, Rev. Sci. Instrum. **81**, 10D325 (2010).
12. Photek Ltd., St. Leonards-on-Sea, East Sussex, TN38 9NS, United Kingdom.
13. T. J. Murphy, R. E. Chrien, and K. A. Klare, Rev. Sci. Instrum. **68**, 610 (1997).
14. V. Yu. Glebov, C. Stoeckl, T. C. Sangster, S. Roberts, G. J. Schmid, R. A. Lerche, and M. J. Moran, Rev. Sci. Instrum. **75**, 3559 (2004).
15. H. Azechi, M. D. Cable, and R. O. Stapf, Laser Part. Beams **9**, 119 (1991).